The COBRA Fixed-Wing Georeferenced Imagery Dataset

Sajad Saeedi†, Carl Thibault†, Michael Trentini⋆, and Howard Li†

***Abstract*—This paper presents a localization and mapping dataset acquired by a fixed-wing unmanned aerial vehicle (UAV). The dataset was collected for educational and research purposes: to save time in dealing with hardware and to compare the results with a benchmark dataset. The data was collected in standard Robot Operating System (ROS) format. The environment, fixed-wing, and sensor configuration are explained in detail. GPS coordinates of the fixed-wing are also available as ground truth. The dataset is available for download [1].**

Index Terms- Fixed-wing, Unmanned Aerial Vehicle, Target Localization, Simultaneous Localization and Mapping (SLAM).

I. Introduction

Aerial robotic systems are developing very rapidly; however, there are key requirements in real-world applications which without them no autonomy can be achieved. One such requirement is the simultaneous localization and mapping (SLAM). SLAM is a process in which an unknown environment is explored and mapped consistently. The robot placed in an *a priori* unknown or partially known environment builds a map of the environment and also situates itself within the map simultaneously [2], [3]. Image mosaicing and target localization, in the presence of pose and measurement uncertainties, are other challenging problems in aerial robotics.

In recent years, researchers have intensively worked on the development of flying machines capable of performing complicated missions with little human supervision. These vehicles are commonly known as unmanned aerial vehicles (UAVs). UAVs have no crew onboard and are flown either remotely by a pilot at a ground control station or autonomously through a pre-planned program. Rotorcraft, such as quadrotors, and fixed-wing aircrafts have attracted more attention recently. In the past decade, for SLAM and target localization using these small flying machines, important advancements have been made. For instance for quadrotors, target localization and SLAM algorithms have been proposed in [4] and [5]. For fixed-wing aircrafts also many algorithms have been presented [6], [7] and [8]. Fixed-wing aircraft and quadrotors have many different applications such as search and rescue [9], agile load transportation [10], and payload dropping [11].

In addition to perception, other problems such as control and state estimation are constantly investigated by researchers. Haryono et al. propose a dual mode fault tolerant algorithm to deal with faults caused by the solar radiation where the frequency of the occurrence of the radiation switches the mode of the algorithm [12]. Wilburn et al. study several different UAV trajectory tracking algorithms in different flight conditions and investigate an adaptation mechanism for UAV control algorithms with fault-tolerant capabilities [13]. Ding et al. propose a UAV system with autonomous formation flight algorithm [14]. The proposed algorithm uses the augmentation algorithm, based on the extended Kalman filter, to cope with the impact of the loss of the wireless data link. Ailneni et al. propose an architecture for UAVs to fuse data from an inertial navigation system and the global positioning system, where the fusion is performed using an extended Kalman filter and a nonlinear complementary filter [15]. Santos et al. use a single camera and the 3D CAD model of a UAV to estimate the pose of the UAV [16].

While there are various algorithms and applications for localization, mapping, image processing, and state estimation; lack of a reliable, complete, and accurate dataset under popular and growing standards is a major issue for researchers. As it will be explained in detail, this paper overcomes these limitations by presenting a new and complete aerial dataset using a well-known robotic messaging standard.

This paper presents an aerial and georeferenced localization and mapping dataset collected at the University of New Brunswick by the COllaboration Based Robotics and Automation (COBRA) group. The dataset can be used for target localization, SLAM, and image mosaicing. The data was collected to assist algorithm developments and help researchers to compare their results. Robotic datasets are specifically important when they are related to unmanned systems such as fixed-wing aircraft.

The dataset in this paper was collected using a fixed-wing aircraft. It was collected in two different configurations. Each configuration includes the same sensors such as pressure sensor, inertial measurement unit (IMU), camera, and global positioning system (GPS); however, the flight patterns are different. Each reading in the dataset was timestamped with a synchronized clock. The dataset is available for download [1].

The Robotics Data Set Repository (RADISH) by A. Howard and N. Roy [17] hosts 41 well-known datasets with different sensors; however, there is no fixed-wing dataset in RADISH. Smith et al. present a visual and laser dataset collected by a ground robot in the Oxford New College campus [18]. Leung et al. present a multiple-robot dataset collect with ground robots in an indoor environment equipped with the VICON position system [19]. Lee et al. present a visual dataset for a micro air vehicle [20]. Various other visual datasets are presented in [21] by Visual Geometry Group. Higashino et al.

†COBRA Group at the University of New Brunswick, Fredericton, Canada, http://www.ece.unb.ca/COBRA/, {sajad.saeedi.g, carl.t, howard}@unb.ca

⋆Defence Research and Development Canada-Suffield, Alberta, Canada, Mike.Trentini@drdc-rddc.gc.ca

present a geomagnetic dataset collected in Antarctica using custom designed UAVs [22].

Robot Operating System (ROS) is a de facto platform in robotic automation, localization, and mapping research community; however, there is no well-known benchmark dataset for aerial localization and mapping which includes inertial, visual, and GPS measurements using ROS standards. Other aerial datasets are available, but they are either based on standards such as Open Geospatial Consortium (OGS) Sensor Web Enablement (SWE) [23], or just present visual measurements suitable for applications such as action recognition. VIRAT Video Dataset [24] is an example of action recognition dataset collected by aerial and ground cameras. Kagaru Airborne Vision Dataset is another example which has been collected using the ORCA Robotics [25] package. The datasets presented in this paper is based on the ROS messaging system and helps researchers and developers to access and use the data in the ROS environment without any interfacing to other standards.

The rest of the paper is organized as follows: Section II presents data collection details including the environment, aircraft, and sensors; Section III explains the collected data, and Section IV makes some general conclusions.

II. Data Collection

The dataset was collected in a large open field with an approximate area of $5000\ m^2$. Five colored targets, each $1 \times 1\ m$ and known GPS coordinates, were located in the field. Two different datasets were collected, in which the only difference was the flight pattern of the aircraft. In the first dataset, the aircraft followed a lawn-mowing pattern. In the second dataset, the aircraft followed multiple figure-8 patterns.

A. Aircraft and Sensors

In this work, a commercial fixed-wing aircraft is used. The aircraft is equipped with a sensor suite and a low-power processing unit. In this section, the fixed-wing and the sensors are explained in detail.

1) 7-foot Telemaster Fixed-Wing: The 7-foot Telemaster fixed-wing aircraft is a light-weight and flexible wooden platform developed by Hobby-Lobby (Fig. 1). An onboard processing unit and a sensor suite have been added to the aircraft. The processing unit includes a Gumstix and a USB hub to interface the sensors, as shown in Fig. 2. The sensor suite includes an RGB camera mounted on a pan-tilt unit, an inertial measurement unit, a pressure sensor, and a GPS. All captured data was sent to a ground control station (GSC) and recorded in a file. The camera data was sent to the GCS via a 1-watt wireless transmission channel, data from the rest of the sensors was transmitted to the GCS using a WiFi modem. Detailed information about the sensors is presented in the following sections.

2) RGB Camera: For imagery data, a BTC-88 Micro Pan/Tilt unit was used [26]. The unit includes a Sony block camera, model FCB-IX11A. It outputs digital images at 30 frames per second. The frames were converted to analogue video and transmitted via a wireless channel to the GCS, where a frame grabber was used to capture 20 frames per second and record them on the computer. The camera was mounted upside down. Fig. 3 shows the mounted camera.

Fig. 1. The 7-foot Telemaster fixed-wing aircraft used for the data collection.

3) Wireless Transmission: To transmit the imagery data to the GCS, first the image frames were converted to NTSC format, then the analogue images were transmitted to the GCS using a wireless channel. On GCS, a Sensoray 2255S frame-grabber was used to captures bit-map images from the analogue imagery at 20 Hz. Fig. 4 shows both the wireless receiver and the frame-grabber.

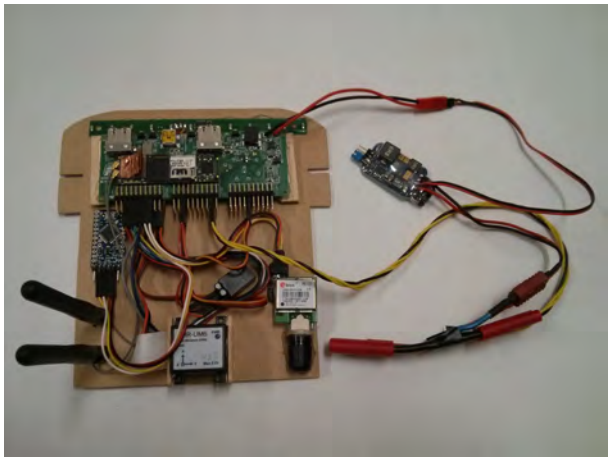

Fig. 2. Onboard sensors and the processing unit. As shown in the figure, the IMU, GPS, and pressure data are captured by the processing unit and sent to the GCS using the WiFi channel. (Camera is not shown in this figure).

4) Inertial Measurement Unit: To measure 3D orientation of the aircraft, the CH Robotics UM6 IMU, which is a light weight orientation sensor, was used [27]. It operates at 500 Hz and includes rate gyros, accelerometers, and magnetic sensors. The data from these sensors were filtered using an extended Kalman filter (EKF), and the results which include the Euler angles were sent to the GCS .

5) Global Positioning System: To acquire GPS measurements, the ublox LEA -5H module, integrated with a u-blox wireless module, was used [28].

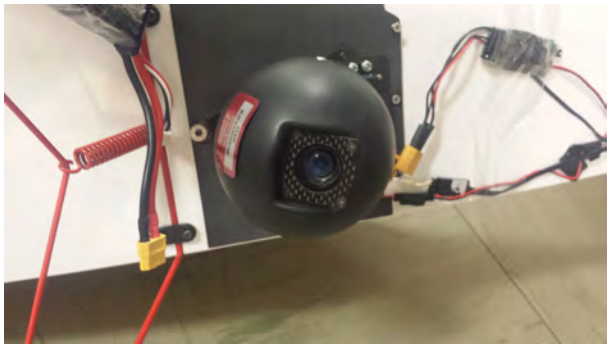

Fig. 3. A Sony block camera mounted underneath the aircraft pointing downwards.

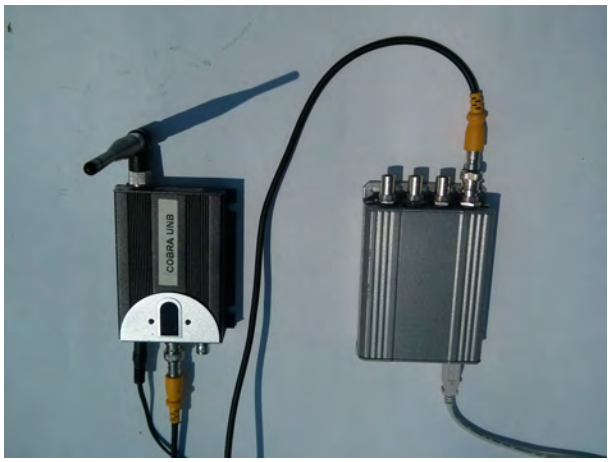

Fig. 4. A wireless receiver (left), and a frame-grabber (right) are used to receive the imagery data.

6) Pressure Sensor: To measure barometric pressure and temperature, BMP085 from Bosch was used [29]. It is interfaced to the processing unit using I2C.

7) Power Monitoring Sensor: To monitor the voltage of the batterey, AttoPilot 90A was used [30].

B. Data Structure and Data Access

In this section, time synchronization, data format, and data access are explained.

1) Time Synchronization: Each measurement has a time-stamp which indicates the time that the data was acquired. The camera data was time-stamped based on the time of the GCS. All other sensors were time-stamped based on the onboard processing unit. Therefore, in order to account for transmission delays, the clocks on the GCS and the onboard processing unit must be synchronized. To synchronize time on the aircraft and the GCS, Chrony [31] was used. Chrony supports online and offline time adjustment by two different applications. In the online case, a Network Time Protocol (NTP) daemon runs in the background and synchronizes the time with time servers. For an isolated machine, one might enter the time periodically. For this work, the clock on the GCS was assumed to be the server clock, and the clock of the onboard processing unit was adjusted based on the server clock. The synchronized time appears as a label in the header of each acquired data.

2) Data Format: The collected datasets were organized using ROS data formats. The captured data is available under a ROS *topic* name. Each reading in the topic starts with a header which indicates the time of the data acquisition. At the end, the sensed data is printed.

Each captured measurement is structured according to Table I. The string of data starts with a header. The first three records, ϕ, θ, and ψ , are inertial measurements using Euler angles, representing roll, pitch, and yaw angles of the aircraft respectively. Then the battery voltage is given. The next eight records are GPS measurements. These records include latitude, longitude, altitude, velocities in the North-East-Down (NED) coordinate system, GPS time, and the error type. Finally the remaining variables are the air pressure and temperature.

TABLE I
MESSAGE FORMAT.

data type	name	description
std_msgs/Header	header	timestamp
float64	phi	inertial measurement, ϕ (rad)
float64	the	inertial measurement, θ, (rad)
float64	psi	inertial measurement, ψ, (rad)
float64	battery_voltage	battery voltage (volt)
float64	lat	GPS latitude (rad)
float64	lon	GPS longitude (rad)
float64	alt	GPS altitude (m)
float64	vn	GPS velocity, in the North direction (m/s)
float64	ve	GPS velocity, in the East direction (m/s)
float64	vd	GPS velocity, sin the Down direction (m/s)
float64	ITOW	GPS ITOW (s)
float64	err_type	GPS error type
float64	pt	air pressure
float64	p_temp	temperature

The topic name for the message in Table I is *cobra_intf*. This topic can be used in any application as presented. Also it can be read and parsed into different sensor messages. A ROS package, called *cobra_sensor_parser*, is developed and accompanied the dataset that subscribes to the *cobra_intf* topic and outputs three separate ROS topics including *imu*, *gps*, and *pss* topics.

To record and replay the data, *rosbag* package [32] is used. Rosbag is designed to have high performance. It also avoids deserialization and reserialization of messages. This package records data from sensors into a file. The file is called *rosbag*. One can easily record/replay a dataset using command-line tools. It is also possible to work with the bagfile using APIs.

III. DATASET

The data collection environment, known as the Durham field, is a large field located in Fredericton, New Brunswick, Canada. Five 1×1 m paper targets with different colors including yellow, green, black, red, and white were placed in different places of the field. Additionally, two red and white cars were in the field and can be considered as two extra targets. As ground-truth data, for each target, GPS coordinates and camera measurements were recorded. The ground-truth information for each target was recorded in a separate file. The

same sensor suite was used to capture ground-truth, while the sensor suite was right on top of the target and was stationary. Fig. 5 shows the field and GPS coordinates of the targets marked with colored markers.

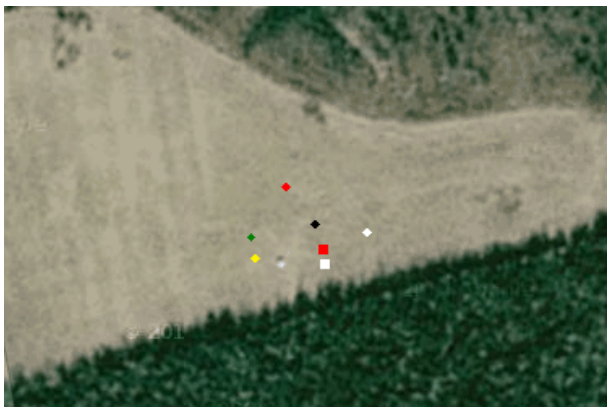

Fig. 5. Georeferenced targets: five small colored points are colored paper targets, and the two bigger squares are two cars. Image from Google Maps.

Fig. 6. GPS trajectory of the first dataset, lawn mowing pattern. Image from Google Maps.

Fig. 7. GPS trajectory of the second dataset, figure-8 motion. Image from Google Maps.

Two different datasets were recorded by the fixed-wing. Both datasets belong to the same environment; however, the trajectories of the fixed-wing in the datasets are different. In the first dataset, the trajectory of the aircraft is a lawn mowing pattern. The ground-truth trajectory, based on the GPS coordinates, is shown in Fig. 6. In the second dataset, the aircraft followed a figure-8 pattern. This motion was repeated three times, so that multiple measurements from the targets were made. Fig 7 shows this pattern.

IV. Conclusion

In this work, two different datasets, collected by a fixed-wing aircraft, were presented. The datasets include sensor readings of the following sensors: camera, GPS, IMU, air pressure, and temperature sensor. The dataset was presented using the ROS messaging format, which provides researcher with various capabilities such as playing the dataset at various rates, pausing dataset, and dropping data. The datasets were collected to help researchers develop and verify their aerial SLAM, image mosaicing, and target localization algorithms. The GPS coordinates of the fixed-wing and targets can be used to verify the results.

In the future, it is desired to extend the work towards multiple homogenous fixed-wings and multiple unmanned aerial and ground systems. Additionally, it is desired to combine indoor and outdoor environments in the datasets including the transition from outdoor to indoor environments and vice versa.

Acknowledgement

This research is supported by Natural Sciences and Engineering Research Council of Canada (NSERC) and Canada Foundation for Innovation.

References

[1] Accessed: 2015-01-02. [Online]. Available: http://www.ece.unb.ca/COBRA/open_source.htm

[2] S. Thrun, W. Burgard, and D. Fox, *Probabilistic Robotics*. Cambridge, Massachusets, USA: The MIT press, 2005.

[3] T. Nakamura and S. Suzuki, "Simplified EKF-SLAM by combining laser range sensor with retro reflective markers for use in kindergarten," *International Journal of Robotics and Mechatronics*, vol. 1, no. 1, pp. 1–7, 2014.

[4] A. Bachrach, R. He, and N. Roy, "Autonomous flight in unknown indoor environments," *International Journal of Micro Air Vehicles*, vol. 1, no. 4, pp. 217–228, December 2009.

[5] S. Grzonka, G. Grisetti, and W. Burgard, "A fully autonomous indoor quadrotor," *IEEE Transaction on robotics*, vol. 28, no. 1, pp. 90–100, February 2012.

[6] M. Warren, D. McKinnon, H. He, A. Glover, M. Shiel, and B. Upcroft, "Large scale monocular vision-only mapping from a fixed-wing sUAS," vol. 92, pp. 495–509, 2014.

[7] M. Bryson and S. Sukkarieh, "Building a robust implementation of bearing-only inertial SLAM for a UAV," *Journal of Field Robotics*, vol. 24, no. 1-2, pp. 113–143, 2007.

[8] J.-H. Kim and S. Sukkarieh, "Airborne simultaneous localisation and map building," in *IEEE International Conference on Robotics and Automation(ICRA)*, vol. 1, 2003, pp. 406–411.

[9] T. Tomic, K. Schmid, P. Lutz, A. Domel, M. Kassecker, E. Mair, I. Grixa, F. Ruess, M. Suppa, and D. Burschka, "Toward a fully autonomous UAV: Research platform for indoor and outdoor urban search and rescue," *Robotics Automation Magazine, IEEE*, vol. 19, no. 3, pp. 46–56, September 2012.

[10] I. Palunko, P. Cruz, and R. Fierro, "Agile load transportation : Safe and efficient load manipulation with aerial robots," *Robotics Automation Magazine, IEEE*, vol. 19, no. 3, pp. 69–79, September 2012.

[11] G. Hadi, R. Varianto, B. Trilaksono, and A. Budiyono, "Autonomous UAV system development for payload dropping mission," *Journal of Instrumentation, Automation and Systems*, vol. 1, no. 2, pp. 72–77, 2014.

[12] H. Haryono, J. Istiyanto, A. Harjoko, and A. Putra, "Technical implementation of dual mode fault tolerance," *Journal of Instrumentation, Automation and Systems*, vol. 1, no. 1, pp. 10–17, 2014.

[13] B. K. Wilburn, M. G. Perhinschi, H. Moncayo, O. Karas, and J. N. Wilburn, "Unmanned aerial vehicle trajectory tracking algorithm comparison," *International Journal of Intelligent Unmanned Systems*, vol. 1, no. 3, pp. 276–302, 2013.

[14] Y.-R. Ding, Y.-C. Liu, and F.-B. Hsiao, "The application of extended kalman filtering to autonomous formation flight of small UAV system," *International Journal of Intelligent Unmanned Systems*, vol. 1, no. 2, pp. 154–186, 2013.

[15] S. Ailneni, S. K. Kashyap, and N. Shantha Kumar, "INS/GPS fusion architectures for unmanned aerial vehicles," *International Journal of Intelligent Unmanned Systems*, vol. 2, no. 3, pp. 154–167, 2014.

[16] N. P. Santos, F. Melcio, V. Lobo, and A. Bernardino, "A ground-based vision system for UAV pose estimation," *International Journal of Robotics and Mechatronics*, vol. 1, no. 4, 2014.

[17] A. Howard and N. Roy, "The robotics data set repository (RADISH)," 2003, accessed: 2015-01-02. [Online]. Available: http://radish.sourceforge.net/

[18] M. Smith, I. Baldwin, W. Churchill, R. Paul, and P. Newman, "The New College vision and laser data set," *The International Journal of Robotics Research*, vol. 28, no. 5, pp. 595–599, May 2009.

[19] K. YK Leung, Y. Halpern, T. Barfoot, and H. HT Liu, "The UTIAS multi-robot cooperative localization and mapping dataset," *International Journal of Robotics Research*, vol. 30, no. 8, pp. 969–974, 2011.

[20] G. H. Lee, M. Achtelik, F. Fraundorfer, M. Pollefeys, and R. Siegwart, "A benchmarking tool for MAV visual pose estimation," in *Control Automation Robotics Vision (ICARCV), 2010 11th International Conference on*, 2010, pp. 1541–1546.

[21] Accessed: 2015-01-02. [Online]. Available: http://www.robots.ox.ac.uk/~vgg/data/

[22] S. Higashino and M. Funaki, "Development and flights of ant-plane UAVs for aerial filming and geomagnetic survey in Antarctica," *Journal of Unmanned System Technology*, vol. 1, no. 2, pp. 37–42, 2013.

[23] C. Reed, M. Botts, J. Davidson, and G. Percivall, "OGC®; sensor web enablement:overview and high level achhitecture." in *Autotestcon, IEEE*, 2007, pp. 372–380.

[24] S. Oh, A. Hoogs, A. Perera, N. Cuntoor, C.-C. Chen, J. T. Lee, S. Mukherjee, J. Aggarwal, H. Lee, L. Davis, E. Swears, X. Wang, Q. Ji, K. Reddy, M. Shah, C. Vondrick, H. Pirsiavash, D. Ramanan, J. Yuen, A. Torralba, B. Song, A. Fong, A. Roy-Chowdhury, and M. Desai, "A large-scale benchmark dataset for event recognition in surveillance video," in *IEEE Conference on Computer Vision and Pattern Recognition (CVPR)*, 2011, pp. 3153–3160.

[25] A. Brooks, T. Kaupp, A. Makarenko, S. Williams, and A. Oreback, "Towards component-based robotics," in *Intelligent Robots and Systems, IEEE/RSJ International Conference on*, 2005, pp. 163–168.

[26] Accessed: 2015-01-02. [Online]. Available: http://www.microuav.com/btc88

[27] Accessed: 2015-01-02. [Online]. Available: http://www.chrobotics.com/shop/orientation-sensor-um6

[28] Accessed: 2015-01-02. [Online]. Available: http://www.u-blox.com/

[29] Accessed: 2015-01-02. [Online]. Available: http://www.adafruit.com/products/391

[30] Accessed: 2015-01-02. [Online]. Available: https://www.sparkfun.com/products/9028

[31] Accessed: 2015-01-02. [Online]. Available: http://chrony.tuxfamily.org/

[32] Accessed: 2015-01-02. [Online]. Available: http://www.ros.org/wiki/rosbag